Characteristics of fragipan B horizons developed on different parent material in North-Western Italy

Published Version:
Raimondo, E., Falsone, G., D'Amico, M., Stanchi, S., Celi, L., Bonifacio, E. (2019). Characteristics of fragipan B horizons developed on different parent material in North-Western Italy. ARCHIV FÜR ACKER- UND PFLANZENBAU UND BODENKUNDE., 65(3), 308-321 [10.1080/03650340.2018.1501474].

Availability:
This version is available at: https://hdl.handle.net/11585/662138 since: 2019-02-08

Published:
DOI: http://doi.org/10.1080/03650340.2018.1501474

Publisher: Taylor & Francis

Journal: *Archives of Agronomy and Soil Science*

DOI: 10.1080/03650340.2018.1501474

Characteristics of fragipan B horizons developed on different parent material in North-Western Italy

E. Raimondo[a]*, G. Falsone[b], M. D'Amico[a], S. Stanchi[ac], L. Celi[a], E. Bonifacio[ac]

Author affiliations.

[a] DISAFA, University of Torino, Largo P. Braccini 2, 10095 Grugliasco, TO, Italy

[b] DISTAL, Alma Mater Studiorum University of Bologna, via Fanin 40, 40127 Bologna, Italy

[c] NATRISK, Research Centre on Natural Risks in Mountain and Hilly Environments, University of Torino, Largo P. Braccini 2, 10095 Grugliasco, TO, Italy

*Corresponding author.

Email address: elisa.raimondo@unito.it (E. Raimondo)

Abstract

A Fragipan (Bx) is a soil horizon hard when dry and brittle when moist, that undergoes slaking upon water immersion, forming a barrier to roots and limiting land use. Brittleness and slaking depend on soil porosity and particle arrangement, but still no agreement exists on the inorganic components responsible for such arrangement. We hypothesized that the same kind of particle arrangement may originate from different soil components, ultimately depending on the lithology of parent material, and evaluated the soil and clay characteristics that best differentiate Bx from B horizons. Thirty-six samples were taken from Typic Fragiudalfs developed on the two sides of an alluvial fan characterized by different amounts of ultramafic materials. Discriminant Analysis evidenced that pedogenic Fe oxides were fundamental in discriminating Bx from B horizons on pure ultramafic parent material, while clay mineralogy was more important in soils with less ultramafic materials. In the first case, the association between clay minerals and self-assembling oxides systems may lead to brittleness, while in the second case the higher abundance of kaolinite may contribute to weak associations between pH-dependent sites and negatively charged surfaces. The only common feature to fragipans on both river sides was a higher degree of weathering.

Keywords: Brittleness, Clay mineralogy, Zeta potential, Weathering, Ultramafic rocks**.**

Introduction

A fragipan is a deep soil horizon that is hard when dry and brittle when moist, whose clods immediately slake when immersed in water. It also has high bulk density (up to 2 kg dm^{-3}), low porosity and large amounts of non-interconnected residual pores (e.g. Wilson et al. 2010). Because of these characteristics, fragipan severely limits plant growth by impeding root penetration, causing failures in seedlings emergence, and interfering with water flow; thus it globally decreases productivity and limits land use (e.g. Daniells 2012). This problem is common to several mid-latitude regions where fragipans occur in Alfisols, Ultisols, Inceptisols and Spodosols (Bockheim and Hartemink 2013). In Europe, fragipan horizons have been described both in Northern and Central countries (e.g. UK, Belgium, the Netherlands, France, Poland, Ukraine) and in Mediterranean ones (e.g. Spain and Italy), but no specific systematic survey is available. In Northern Italy they are mostly found in Alfisols or Ultisols developed on Middle Pleistocene fluvioglacial terraces (e.g. Ajmone-Marsan and Torrent 1989, Falsone and Bonifacio 2006). When they are not cultivated with rice or other crops, they host the remnants of the native forests that once covered the Po plain. Fragipans and/or fragic properties also occur in Apennine Paleosols (Costantini et al. 1996; D'Amico et al. 2016) and discontinuously in some forest Inceptisols of Central Italy (Certini et al. 2007).

Both the USDA Soil Taxonomy (Soil Survey Staff 2014) and the World Reference Base for Soil Resources (IUSS Working Group WRB 2014) recognize fragipans on the basis of their morphology and slaking field tests.

The origin of fragipan brittleness is still debated, and two groups of theories are widely discussed. The first group emphasizes physical processes, i.e. self-weight collapse followed by physical ripening (e.g. Bryant 1989), or frost heaving and other periglacial conditions (Van Vliet and Langohr 1981) that allow a close-packing of soil grains and induce the typical high bulk density. However, not all soils that have experienced those physical processes have developed a fragipan, suggesting that specific soil phases are necessary for reversible cementation and brittleness. The second group of theories stresses instead the role of chemical bonding between mineral grains, but there is no agreement on the nature of such bridges. Some researchers suggested that they are composed by clay minerals (e.g. Habecker et al. 1990), others claimed the involvement of poorly-crystalline silicates (e.g. Ajmone-Marsan and Torrent 1989; Park et al. 2006), and other authors (e.g. Hallmark and Smeck 1979) stated that the bridges are composed by Fe and/or Si and Al oxides. It seems therefore that several inorganic components may originate the same kind of morphological characteristics and convincing evidences about both a physical and a chemical origin are reported.

Despite the lack of agreement on fragipan genesis, there is a general consensus that physical arrangement of particles and pore size distribution play a crucial role in fragipan behavior upon water saturation, i.e. on the most typical morphological characteristic. Assuming that slaking is indeed caused by the rapid substitution of the air entrapped into the smallest pores with water (Sole´ et al. 1992), a specific relation between the arrangement of silt and clay (Aide and Marshaus 2002) or among clay particles (Falsone and Bonifacio 2006) has been hypothesized. The fragipan showed in fact an open packing of the clay phase, associated with an extremely dense packing of silt and sand (Falsone and Bonifacio 2009). The way particles associate to each other depends on the surface properties of the clay fraction (both silicate and non-silicate phases), and on the concentrations of cations in the soil solution (Zhang and Norton 2002). Clay mineralogy could therefore have a fundamental role in determining the characteristics of the fragipan, by shaping the interactions between particles, both in the case of physical compaction and of chemical bonding.

The characteristics of clay minerals and other inorganic phases strongly depend on the pedogenic processes that have occurred under the influence of soil forming factors. While it is well known that fragipan distribution is preferentially related to soil age, climate, latitude, soil texture and vegetation (Bockheim and Hartemink 2013), less is reported about the effect of soil parent material. Fragipans occur on mixed lithologies such as medium-textured, acidic glacial drift and colluvium but also on lacustrine materials, alluvium or loess parent material (e.g. Bockheim and Hartemink 2013; Witty and Knox 1989), showing therefore little specificity. In NW Italy they also occur on ultramafic alluvial materials as reported by Falsone and Bonifacio (2006).

Because of the large amount of differing evidences about the main factors inducing fragipan characteristics, we hypothesized that a similar association between soil particles may originate from several soil mineral phases, ultimately depending on the parent material. Only a set of properties may thus allow to identify fragipan horizons from the chemical and mineralogical point of view. The aims of this work were therefore: a) to evaluate fragipan morphological, chemical and mineralogical characteristics in soils developed on two different parent materials in a relatively small area in North-Western Italy; b) to identify the set of properties related to the soil and clay phases that differentiate fragipan from non-fragipan B horizons, and finally; c) to assess if fragipans developed on different parent materials display some common features.

Materials and methods

Study area and soil sampling

The study area is a part of the Stura di Lanzo alluvial fan, in North-Western Italy (Figure 1A). This Pleistocene terraced fan is preserved from the Alpine range into the Po plain at an altitude between 210 and 550 m a.s.l. and it has an extension of about 300 km^2. Both sides of the fan are characterized by several orders of flat to gently undulated terraces formed during the Pleistocene glaciations and separated by embankments of 2-20 m. The left river side is composed of fluvio-glacial and alluvial materials mainly derived from the inputs of the Stura di Lanzo river (a tributary of the Po river), whose watershed is characterized by ca. 60% ophiolitic outcrops (serpentinites and peridotites of the Piedmont ophiolite system) and ca. 40% sialic gneiss belonging to the Sesia-Lanzo zone. The right river side is influenced by abundant ultramafic inputs derived from the Ceronda river, whose basin is completely carved into the Lanzo Ultrabasic Complex (Servizio Geologico d'Italia 2009). A different mineralogy of the soil parent material is therefore expected on the two river sides and, consequently, different soil properties. To evaluate the effect of the parent material on soil properties, we selected sampling sites on both sides of the fan.

The climatic conditions of all sites are comparable, and the soil temperature and moisture regimes are mesic and udic, respectively (IPLA, 2009).

During a soil survey campaign, six Typic Fragiudalfs (Soil Survey Staff 2014) were selected for this study (Figure 1B). Three of them were on the right river side (P1; P2; P3) and three on the left side (P4; P5; P6) as visible in Table 1. They all developed on Mindel (MIS 12) fluvio-glacial and alluvial terraces (Forno et al. 2007). Soil profile description was carried out following the FAO guidelines (2006). In this work we considered only the B horizons (fragipan and non-fragipan), which were thirty-six in total.

Some preliminary analyses were carried out to verify that the soil properties mostly affected by the parent material differed between the two river sides. We took into account the concentration of total Fe and the amounts of smectite, both expected to be higher on soil derived from pure ultramafic materials (e.g. Hseu et al. 2007). The analytical methods were the same as described in the next paragraph. All B horizons (fragipan and non-fragipan) sampled on the right river side showed a higher total Fe content (76.5 ± 36.6 g Kg^{-1} vs 46.3 ± 15.4 g Kg^{-1}, n = 36, $p < 0.01$), and a significantly higher abundance of smectite (9.7 ± 10.2 % vs 1.4 ± 3.4 %, n = 36, $p < 0.05$) in the clay fraction, confirming the expected differences.

Chemical and mineralogical analyses

The thirty-six samples were air dried, sieved at 2 mm and analyzed according to the methods reported by Van Reeuwijk (2002). The pH was determined potentiometrically in a water suspension (1:2.5 w/w); the organic C (OC) content was measured by dry combustion (NA 2100 Protein elemental analyzer, CE Instruments, Rodano, Italy). The particle-size distribution was measured by the pipette method, determining the amount of coarse sand by wet sieving. The cation exchange capacities (CEC) was determined by the $BaCl_2$-triethanolamine method and the exchangeable bases (Ca_{ex}, Mg_{ex}, K_{ex}) were measured by atomic absorption spectrophotometry (Perkin Elmer, Analyst 400, Waltham, MA, USA). Acid ammonium oxalate and Na-dithionite-citrate-bicarbonate were used to extract Fe, Mn, Si, Al (Fe_O, Fe_D, Mn_O, Mn_D, Si_D and Al_O) from pedogenic forms. Mn was also extracted with hydroxylamine-HCl (Mn_H). The total element concentrations (Fe_T and Mn_T) were determined after hot HCl-HNO_3 (3:1) treatment. The Fe, Mn, Si and Al concentrations in the extracts were measured by atomic absorption spectrophotometry.

The clay fraction (< 2 μm) was dispersed in water, separated by sedimentation and freeze-dried for the mineralogical and electrophoretic mobility investigations. The mineralogical analyses were carried out using a Philips PW1729 X-ray diffractometer (40 kV and 20 mA, Co Kα radiation, graphite monochromator) on clay oriented mounts. Scans were made from 3 to 35° 2θ at a speed of 1° 2θ min^{-1}, on air dried Mg-saturated (AD), ethylene glycol solvated (EG), and heated (550 °C) samples. The identification of clay minerals was done by comparing peak position and intensity in all XRD patterns, as described in Falsone et al. (2012). Associated minerals (quartz, talc and feldspars) were identified by peak positions according to the data reported by Brown (1980). A semi-quantitative evaluation of mineral abundance was performed using the Mineral Intensity Factors method reported by Islam and Lotse (1986) that takes into account peak areas and is suitable for oriented samples. For the analysis, the background was subtracted and the peak positions, intensities and areas were calculated using the second derivative option of the PowderX software (Dong, 1999). The abundance of clay phyllosilicates was summarized with the Equivalent Basal Spacing (EBS) proposed by Schmitz et al. (2004): this index increases with increasing contents of swelling or 1.4 nm layer silicates.

The zeta potential (ζ), an estimate of clay surface charge, was calculated from the electrophoretic mobility by Laser Doppler Velocimetry coupled with Photon Correlation Spectroscopy (LDV-PCS) using a spectrometer (DELSA 400, Beckman Coulter Inc. Hialeah, FL) equipped with a 5 mW He–Ne laser (632.8 nm). The analysis was carried out on clay suspensions at the soil pH, using a 1:100 clay to 0.01 M NaCl ratio.

Statistical analyses

All statistical analyses were carried out with SPSS v24.0. The differences in chemical and mineralogical properties between the fragipan and non-fragipan B horizons were evaluated by one-way ANOVA using a significance level of $p < 0.05$ after Levene's homoscedasticity test. The simultaneous effect and the relative contribution of soil or clay properties that differentiate fragipan from non-fragipan B horizons were evaluated through Discriminant Analysis. Variables were inserted stepwise and the goodness of the discrimination was evaluated using the canonical correlation, with a threshold of 0.5 as good discrimination. The proportion of variance explained by the discriminant function was assessed with the

Eigenvalue and the Wilks' Lambda coefficient. The variable contribution to the discrimination was evaluated using the standard coefficients of the canonical discriminant function. The global goodness of the Discriminant Analysis was assessed through the re-classification of the data, using a cross-validation method.

Results

Morphological, chemical and mineralogical characteristics of fragipan and non-fragipan B horizons of the right river side (pure ultramafic materials)

Fragic soil properties were well expressed in Bcx (P1, P2, P3), Btcx (P1) and Btx (P2, P3) horizons on this river side (Table 2), below Btc (P1), Bw (P2) or Bwg (P3) horizons. At the top of the profiles, A horizons were always found (Figure 1B). The color of non-fragipan horizons was typically yellowish brown to olive brown (10YR - 2.5Y) with frequent black mottles (2.5Y 2.5/1), while fragipan color ranged from yellowish brown to reddish brown (10YR – 5YR), with red (e.g. 10R 4/8 or 5YR 5/), grey (2.5Y 7/1 or 5/2) and dark mottles (2.5Y 2.5/1). All non-fragipan B horizons showed a blocky angular or subangular structure while Bx instead had platy or blocky angular structure (Table 2). The thickness of the fragipan B horizons varied among profiles, and the boundary between fragipans and non-fragipans was generally smooth and ranged from abrupt to gradual. All fragipans had a firm to very firm consistence. They were hard when dry and brittle when moist, and underwent slaking upon water saturation.

On this river side, fragipan (Bx) and non-fragipan (B) horizons differed in particle size distribution (Table 3): Bx horizons had more clay ($p < 0.05$) and less silt ($p < 0.05$) than the other B horizons, while the percentage of sand was not significantly different. The CEC was higher in Bx horizons ($p < 0.01$), as well as the amounts of both exchangeable Ca ($p < 0.01$) and Mg ($p < 0.05$). Differences between genetic horizons were also visible in geochemical properties, with higher amounts of Fe_T and Fe_D ($p < 0.01$), and higher Si_D in fragipans (p <

0.05). In non-fragipan B horizons the Fe_O/Fe_D ratio was 0.05 ± 0.02 and Fe_D/Fe_T 0.52 ± 0.10 on average; in fragipans the proportion of poorly crystalline Fe oxides was lower ($p < 0.01$) and the Fe_D/Fe_T was 0.59 ± 0.18. The clay fraction from Bx horizons was characterized by the abundance of irregular interstratified minerals and the presence of partially weathered forms of illite and chlorite, as visible from the broad peaks in the XRD pattern (Figure 2A). Chlorite, in particular, was characterized by a sharp peak after heating in most non-fragipan B horizons, while in Bx horizons it was often completely transformed to hydroxyl-interlayered vermiculite (or chlorite-vermiculite mixed layers). From the semi-quantitative point of view, chlorite and chlorite-mixed layer minerals were significantly less abundant in fragipans than in the other B horizons (Figure 3A, $p < 0.05$). Although the variability was large, fragipans had a significantly higher EBS (Table 3, $p < 0.05$), but the zeta potential did not show significant differences (Table 3). On this river side, a good discrimination between B and Bx horizons ($p < 0.001$) was obtained through a function that used 2 soil variables (Table 4): pedogenic Fe oxides (Fe_D) and K_{ex}. This discriminant function fully explained the sample variance, and the Eigenvalue (2.50, Table 4) indicated a high ratio between between-groups and within-groups sum of squares. The standardized coefficients of the discriminant function indicated a comparable effect of the variables in discrimination. The reclassification was very good (95%). The only clay characteristics retained in the discrimination between fragipan and non-fragipan horizons of the right river side were the amounts of chlorite-vermiculite mixed layer minerals (i.e. 14-14 in Table 4) and of illite-containing irregular interstratified minerals (10-14 in Table 4, i.e. illite-vermiculite, illite-chlorite). This discriminant function totally explained the sample variance, but the Eigenvalue was much lower than the one obtained by using soil properties, and the Wilks'lambda was 0.57 (Table 4). However, the reclassification was still satisfactory good (84%).

Morphological, chemical and mineralogical characteristics of fragipan and non-fragipan B horizons of the left river side (ultramafic and sialic materials)

Fragic properties were recognized in Btx (P4, P5, P6), Bcx (P4) and Bwx (P6) horizons on this left river side, below E (P4), Btc (P5) or Bwg (P6) horizons (Table 2). The fragipan horizons were similar to those found on the opposite river side in color (from yellowish brown to reddish brown, with frequent mottles, Table 2), and structure (platy or angular blocky).

Fragipan and non-fragipan horizons were more similar than on the opposite river side (Table 3). The horizons did not significantly differ in particle size distribution, and among chemical properties, they only differed in the amounts of exchangeable K, which was lower in fragipans ($p < 0.05$). All differences related to Fe, Si and Mn forms that were significant on the right river side, were not present on this river side, although the contents were always slightly higher in fragipans. Fragipan and non-fragipan horizons had more differences in clay mineralogy. As on the opposite river side, chlorite was more weathered in Bx than in B horizons; in addition, some fragipans contained irregular swelling mixed layer minerals (Figure 2B). The semiquantitative analysis (Figure 3B) showed that fragipan horizons were characterized by lower amounts of chlorite (6% in B and 2% in Bx on average, $p < 0.05$), higher ($p < 0.05$) contents of vermiculite (24% vs 33% in B and Bx, respectively) and kaolinite (30% in B and 38% in Bx). Despite these differences, the EBS did not differ (Table 3). The zeta potential did not significantly differ either (Table 3). In contrast with the findings obtained for the opposite river side, a better discrimination between fragipan and non-fragipan was obtained using clay properties rather than soil properties. The discriminant function built using soil properties took into consideration only the cation exchange capacity and the amounts of exchangeable K. The goodness of reclassification was 88%, with acceptable Eigenvalues and Wilks'lambda coefficient (Table 4). Several clay minerals were instead retained in the clay discriminant function: kaolinite had the highest standardized coefficient, vermiculite and irregular interstratified swelling clay minerals (i.e. chlorite-smectite or vermiculite-smectite) had almost the same standardized coefficients, while smectite weighted less and was negatively correlated to fragipans. The Eigenvalue was above 5, and the samples were perfectly reclassified. Neither on this river side the discriminant functions took into account the zeta potential.

Common features of fragipan and non-fragipan B horizons of both riversides

When the samples of the two river sides were considered as a unique dataset (n = 36), fragipan and non-fragipan B horizons differed in the concentration of organic C, which was lower in Bx horizons ($p < 0.01$), and in particle size distribution ($p < 0.05$) (Table 5). Fragipans showed higher amounts of clay and lower amounts of silt, therefore the Bx horizons were clay loam while B horizons were loam. The Fe (hydr)oxides were significantly more crystalline (i.e. lower Fe_O/Fe_D ratio, Table 5, $p < 0.01$) in Bx horizons, although the abundances were similar. The content of Si_D was higher in fragipans ($p < 0.05$), but the concentration of extractable Al and Mn (all forms) did not differ. No significant differences in clay mineral abundance were visible (data not shown), although the slightly higher contents of vermiculite and smectite lead to higher Equivalent Basal Spacing (EBS) in Bx than in B horizons (Table 5, $p < 0.05$). The zeta potential was around -16.0 mV in non-fragipan and -14.4 mV in fragipan B horizons, and no significant difference was found between B and Bx horizons (Table 5).

Discussion

The presence of fragipan poses well-known problems to land use all over the world, therefore research about their origin dates back to the dawn of soil science (e.g. Daniells 2012). In this work we hypothesized that the many different and convincing evidences reported in the literature about the factors that cause fragipan most typical and problematic characteristics (reversible induration, brittleness and slaking) may be related to the presence of different inorganic soil components that, however, may originate a similar particle arrangement, thus leading to the same morphological features. We assumed that differences in the soil mineral phases were related to differences in the soil parent material (pure ultramafic alluvium on the right river side and ultramafic mixed with sialic materials on the left river side), and aimed at identifying the properties that discriminated fragipan from non-fragipan B horizons. We took into account both the soil properties that may affect the reversible cementation, and the clay characteristics that can influence the physical arrangement of the clay phase. We also aimed at evaluating if there are some chemical or mineralogical features common to fragipans developed on different parent materials in an otherwise homogeneous study area.

Soil morphology (Table 2) clearly depicted the most typical fragipan characteristics in terms of structure, brittleness, and slaking behaviour (e.g. Bockheim and Hartemink 2013). The color of fragipan B horizons, ranging from 2.5Y to 10YR, indicated the dominance of goethite among Fe (hydr)oxides (color of pure fine goethite is close to 10YR), in agreement with the pedogenic environment (Schwertmann 1993). Mottles indicating fluctuations of redox potential were also abundant in the fragipans (e.g. 40%; Table 2), as found in other works (e.g. Payton, 1993). However, no differences in field morphology were found between fragipans developed on the right and the left river sides that always matched the USDA Soil Taxonomy (Soil Survey Staff 2014) and the World Reference Base for Soil Resources (IUSS Working Group WRB 2014) requirements.

The group of variables that better discriminated Bx from B horizons varied between river sides, suggesting a marked effect of the soil parent material. On the right river side, soil properties were more effective in the discrimination, while on the left river side the characteristics of the clay fraction had a greater effect in the differentiation of B horizons.

On the right river side, fragipan presence was correlated to a higher content of pedogenic Fe (hydr)oxides and more exchangeable K than in non-fragipan B horizons. All soils developed on this river side were Fe-rich (Fe_T = 76.5 g kg^{-1} on average, as described in the study area section) because of pure ultramafic parent material, thus high amounts of Fe oxides were expected to form during pedogenesis (e.g. Hseu et al. 2007). However, despite the general abundance, fragipans were richer in Fe_D than non-fragipans horizons (Table 3). The Fe_D

concentration was much higher than those commonly found in literature (e.g. Ajmone-Marsan and Torrent 1989, Duncan and Frenzmeier 1999) but, to the best of our knowledge, there are no previous reports of fragipans on other ultramafic areas. The higher content of pedogenic Fe oxides indicates a more advanced stage of weathering of Bx horizons, but also suggests a possible effect on particle aggregation. Increasing concentrations of Fe oxide nanoparticles promote their aggregation (Baalousha 2009) and in highly weathered, Fe-rich soils, they typically form microaggregates among themselves instead of coatings on layer silicates (Shang and Tiessen 1998). The interaction between silicates and oxides will thus occur only as a successive step, between self-assembled micrometric oxide units and phyllosilicates, and will therefore be bigger, more porous, and less stable than in the case of surface coating of phyllosilicates by Fe oxides. The slightly larger particle size of the clay fraction from fragipan B horizons measured during the electrophoretic mobility analysis confirmed this hypothesis (B: 963.7 nm ± 155.4; Bx: 1073.0 nm ± 188.6; data not shown). We can therefore, hypothesize that, when positively charged Fe minerals are present in very high concentration in the soil (60.0 g_{FeD} Kg^{-1} ± 31.3 in Bx, Table 3), they can play a role in the reversible cementation and brittleness of fragipan horizons. The inclusion of K in the discriminant equation was somehow surprising, considering that no significant differences in K_{ex} content were observed between B and Bx horizons (Table 3) and the amounts were quite low, as common in soils of Northwestern Italy (Bonifacio et al. 2013). The effect may however be indirect as K_{ex} could be considered as a marker of a more advanced weathering stage of Bx horizons on this river side. The transformation of illite into interstratified minerals and then into vermiculite through the loss of fixed K is a typical mineral transformation in temperate climates (Allen and Hajek, 1989). This transformation is more complete in Bx than in B horizons, as indicated by the very broad XRD band at 1.0 nm (Figure 2A). The indirect effect of K is confirmed by the discriminant function obtained with clay properties; fragipan occurrence on the right river side was indeed positively correlated to illite mixed-layer minerals (Table 4).

On the left river side, where the parent material is less Fe-rich, and the soils have lower amounts of (hydr)oxides, the composition of clay minerals plays a greater role in Bx horizons discrimination. Fragipans were positively correlated to higher contents of vermiculite, swelling mixed layers, and kaolinite, but negatively with smectite. Pedogenic kaolinite is the end-product of K-feldspar or smectite transformations (Wilson 2004), while vermiculite may form from illite through the loss of the interlayer K. These mineral transformations are expected upon advanced pedogenesis and evidence the higher development of fragipans with respect to the non-fragipan B horizons. In addition of being a marker of advanced pedogenesis (Wilson 2004), kaolinite favours fragipan development (Ramos et al. 2015) and may play a role in clay aggregation. Because of its larger pH-dependent charge, the association between the kaolinite positively charged sites and negatively charged 2:1 phyllosilicate surfaces (e.g. Wang and Siu 2006) is probable. This may induce clay phase characteristics similar to those found in the Bx horizons of the right river side: an unstable and highly porous association, bound by electrostatic interaction, that may undergo disruption upon wetting. Although not significantly different between Bx and B horizons, the less negative zeta potential that we found in fragipans (Table 3) confirmed the presence of positively charged kaolinite sites at the soil pH. Interstratified swelling clay minerals contributed in discriminating fragipans from non-fragipans, in agreement with the effect that swelling has on the reversible (i.e. moisture dependent) induration and brittleness (Szymański et al. 2012). However, the smectite contents were negatively correlated with fragipan presence, thus they are either too low (Figure 3) to have an effect in the behavior of these genetic horizons, or the contribution of swelling mixed-layers to the discriminant function is more related to weathering indicators than to an effect of swelling on fragipan behavior. Soil mineralogy also explains the variables that were retained in the discriminant function built using the fine earth properties. Upon an increase of kaolinite, the soil CEC is expected to decrease (Allen and Hajek 1989), as well as the amounts of exchangeable cations. Although the differences were not significant, the CEC calculated on a clay basis varied from 54.8 ± 22.1 $cmol_{(+)}$ Kg^{-1} in Bx to 71.6 ± 22.1 $cmol_{(+)}$ Kg^{-1} in the other B horizons (Table 3).

There are other variables that showed significant differences between fragipan and non-fragipan horizons, which were however not retained in the discriminant functions, particularly on the right river side, such as the organic C and clay contents, several Fe forms, and CEC and exchangeable cations (Table 3). The low organic C content is a typical fragipan characteristic (IUSS Working Group WRB 2014) and explains also the lower Fe_O/Fe_D ratio. The greater CEC in fragipan horizons is likely related to the higher amounts of clay, as kaolinite (the clay mineral with the lowest CEC) did not significantly differ on the right river side. Amorphous forms of Si and Al have been related to fragipan genesis (e.g. Ajmone-Marsan and Torrent 1989; Corrêa et al. 2005; Tremocoldi et al. 1994), mainly because they can act as bonding agents among grains. We found no differences in Al contents, while the amounts of Si_D were significantly higher in Bx horizons of the right river side. The Si_D concentrations were however much lower than those reported by e.g. Steinhardt et al (1982) or Tremocoldi et al. (1994), likely because of the Si paucity of the ultramafic parent material. The effect of extractable Si on fragipan characteristics cannot therefore be identified in this work. Manganese forms did not significantly differ either (Table 3), although the contents were always lower in Bx horizons; this may be related to the redox fluctuations that are recorded in fragipans by the abundance of mottles (Table 2).

Soil parent material had a marked effect on fragipan distinctive chemical and mineralogical characteristics, although on both river sides fragipans were more developed than non-fragipans, in agreement with e.g. Petersen et al. (1970). If both riversides are examined together, the more advanced genetic stage is partially confirmed. All fragipan horizons had higher amounts of clay and lower of silt and sand, and showed a greater crystallinity of Fe oxides (Table 5). Clay contents increase with soil development and, with time, poorly crystalline oxides (Fe_O) evolve to more crystalline forms (Fe_D) (Schwertmann 1993). The higher amounts of clay are not included among the typical fragipan characteristics, but are similar to those found in other works (e.g. Costantini et al. 1996). Furthermore, the study area is characterized by the presence of ultramafic alluvial sediments, which often lead to fine-textured soils (Rabenhorst et al. 1982). The presence of even small inclusions of sialic rocks deeply affect soil development in ultramafic areas (D'Amico et al. 2015), thus the few differences between fragipan and non-fragipan B horizons we found when both river sides were considered together are likely related to an increase in the variability of soil characteristics.

Conclusions

Despite the difference in the parent material lithology, fragipan horizons on both river sides were characterized by similar morphological properties and by a more pronounced weathering stage than the other B horizons. However, even in a relatively small and homogeneous alluvial fan, differences in the composition of the parent material lead to differences among the variables that allowed to statistically differentiate fragipan from non-fragipan horizons. Where abundant Fe oxides originated from the weathering of the pure ultramafic parent material, they became fundamental in discrimination. On the opposite, where the amounts of (hydr)oxides were low, Bx horizons had a different clay mineralogical composition with respect to non-fragipans. No clear indication about the chemical agents promoting fragipan induration was obtained from this work, but on both river sides a weak association within the clay fraction may be responsible for the occurrence of slaking in soils. However, depending on the soil parent material, the mineral phases that are responsible of such association vary. Even if further research is needed to clarify the mechanisms of the suggested processes, our results clearly indicate that different soil components can lead to the same morphological characteristics, reconciling therefore some of the many opinions in a long lasting debate about the chemical responsible of fragipan behavior.

References

Aide, M. and Marshaus, A. 2002. Fragipan genesis in two Alfisols in East Central Missouri. Soil Science 167, 453-464.

Ajmone-Marsan, F. and Torrent, J. 1989. Fragipan bonding by silica and iron oxides in a soil from Northwestern Italy. Soil Science Society of America Journal 53, 1140-1145.

Allen, B.L. and Hajek, B.F. 1989. Mineral occurrence in soil environments. In: Dixon, J.B. Weed, S.B. (Eds.), Minerals in Soil Environments. Soil Science Society of America, 199-278.

Baalousha, M. 2009. Aggregation and disaggregation of iron oxide nanoparticles: Influence of particle concentration, pH and natural organic matter. Science of the Total Environment 407, 2093-2101.

Bockheim, J.G. and Hartemink, A.E. 2013. Soils with fragipans in the USA. Catena 104, 233-242.

Bonifacio, E. Falsone G. Catoni M. 2013. Influence of serpentine abundance on the vertical distribution of available elements in soils. Plant & Soil, 368, 493-506.

Brown, G. 1980. Associated minerals. In: Brindley, G.W. Brown, G. (Eds.), Crystal Structures of Clay Minerals and Their X-ray Identification, Monograph 5. Mineralogical Society, London, 361-410.

Bryant, R.B. 1989. Physical processes of fragipan formation. In: Fragipans: Their occurrence, classification and genesis. N. E. Smeck, and E. J. Ciolkosz (eds.). SSSA Spec. Publ. SSSA, Madison, WI, 141-150.

Corrêa, M.M. Ker, J.C. Araújo Filho, J.C. Camêlo, D.L. 2005. Formas de ferro, silício e, ou, alumínio na gênese de fragipãs e horizontes coesos dos tabuleiros costeiros. Revista Brasileira de Ciência do Solo 39, 940-949.

Costantini, E.A.C. Napoli, R. Bragato, G. 1996. Properties and geographic relevance of fragipan and other close-packed horizons in a non-glaciated Mediterranean region. Geografia Fisica e Dinamica Quaternaria 19, 29-45.

Daniells, I.G. 2012. Cohesive soils: a review. Soil Research 50, 349-359

D’Amico, M.E. Freppaz, M. Leonelli, G. Bonifacio, E. Zanini, E. 2015 Early stages of soil development on serpentinite: the proglacial area of the Verra Grande Glacier, Western Italian Alps. Journal of Soils and Sediments 15, 1292-1310.

D'Amico, M.E. Catoni. M. Terribile, F. Zanini, E. Bonifacio, E. 2016. Contrasting environmental memories in relict soils on different parent rocks in the south-western Italian Alps. Quaternary International 418, 61-74.

Dong, C. 1999. PowderX: Windows-95 based program for powderX-ray diffraction data processing. J. Appl. Crystallogr. 32, 838.

Duncan, M.M. and Franzmeier, D.P. 1999. Role of free silicon, aluminum, and iron in fragipan formation. Soil Science Society of America Journal 63, 923-929.

Falsone, G. and Bonifacio, E. 2006. Destabilization of aggregates in some Typic Fragiudalfs. Soil Science 171, 272-281.

Falsone, G. and Bonifacio, E. 2009. Pore-size distribution and particle arrangement in fragipan and non-fragipan horizons. Journal of Plant Nutrition and Soil Science 172, 696-703.

Falsone, G. Celi, L. Caimi, A. Simonov, G. Bonifacio, E. 2012. The effect of clear cutting on podzolisation and soil carbon dynamics in boreal forests (Middle Taiga zone, Russia). Geoderma 177-178, 27–38.

FAO, 2006. Guidelines for Soil Description, fourth ed. FAO, Rome.

Forno, G.M. Gregorio, L. Vatteroni, R. 2007. La successione stratigrafica del settore destro del Conoide di Lanzo e il suo significato per l'utilizzo del territorio. Memorie Società Geologica Italiana 87, 237–247.

Habecker, M.A. McSweeney, K. Madison, F.W. 1990. Identification and genesis of fragipans in Ochrepts of north central Wisconsin. Soil Science Society of America Journal 54, 139-146.

Hallmark, C.T. and Smeck, N.E. 1979. The effect of extractable aluminum, iron, and silicon on strength and bonding of fragipans of Northeastern Ohio. Soil Science Society of America Journal 43, 145-150.

Hseu, Z.Y. Tsai, H. Hsi, H.C. Chen, Y.C. 2007. Weathering sequences of clay minerals in soils along a serpentinitic toposequence. Clays and Clay Minerals 55, 389-401.

IPLA, 2009. Carta dei suoli del Piemonte 1:50000. Regione Piemonte, S.E.L.C.A. Firenze.

Islam, A.K.M.E. and Lotse, E.G. 1986. Quantitative mineralogical analysis of some Bangladesh soils with X-ray, ion exchange and selective dissolution techniques. Clay Minerals 21, 31-42.

IUSS Working Group WRB, 2014. World Reference Base for Soil Resources 2014. International soil classification system for naming soils and creating legends for soil maps. World Soil Resources Reports No. 106. FAO, Rome.

Park, S.J. Almond, P. McSweeney, K. Lowery, B. 2006. Fragipan formation within closed depression in Southern Wisconsin, United States. Journal of the Korean Geographical Society 41, 150-167.

Payton, R.W. 1993. Fragipan formation in argillic brown earths (Fragiudalfs) of the Milfield Plain, north-east England. II. Post Devensian developmental processes and the origin of fragipan consistence. Journal of Soil Science 44, 703-723.

Petersen, G.W. Ranney, R.W. Cunningham, R.L. Matelski, R.P. 1970. Fragipans in Pennsylvania Soils: A Statistical Study of Laboratory Data. Soil Science Society of America Journal 34, 719-722.

Rabenhorst, M.C. Foss, J.E. Fanning, D.S. 1982. Genesis of Maryland Soils Formed from Serpentinite. Soil Science Society of America Journal 46, 607-616.

Ramos, M.R. Melo, V.F. Uhlmann, A. Dedecek, R.A. Curcio, G.R. 2015. Clay mineralogy and genesis of fragipan in soils from Southeast Brazil. Catena 135, 22-28.

Schmitz, R.M. Schroeder, C. Charlier, R. 2004. Chemo-mechanical interactions in clay: a correlation between clay mineralogy and Atterberg limits. Applied Clay Science 26, 351-358.

Schwertmann, U. 1993. Relations Between Iron Oxides, Soil Color, and Soil Formation. In: Bigham, J. M. and Ciolkosz, E. J. editors, Soil Color. Soil Science Society of America Journal Spec. Publ. 31, 51-69.

Servizio Geologico d'Italia, 2009. Carta geologica d'Italia 1:50000, sheet 134 and notes. Regione Piemonte, Direzione Regionale Servizi Tecnici e di Prevenzione, Torino.

Shang, C. and Tiessen, H. 1998. Organic Matter Stabilization in Two Semiarid Tropical Soils: Size, Density, and Magnetic Separations. Soil Science 62, 1247-1257.

Soil Survey Staff, 2014. Keys to Soil Taxonomy, 11th edition. USDA, National Resources Conservation Service, National Soil Survey Center, Lincoln, NE.

Sole´, A. Josa, R. Pardini, G. Aringhieri, R. Plana, F. Gallart, F. 1992. How mudrock and soil physical properties influence badland formation at Vallcebre (Pre-Pyrenees, NE Spain). Catena 19, 287-300.

Steinhardt, G.C. Franzmeier, D.P. Norton, L.D. 1982. Silica Associated with Fragipan and Non-Fragipan Horizons. Soil Science Society of America Journal 46, 656-657.

Szymański, W. Skiba, M. Skiba, S. 2012. Origin of reversible cementation and brittleness of the fragipan horizon in Albeluvisols of the Carpathian Foothills, Poland. Catena 99, 66-74.

Tremocoldi, W.A. Steinhardt, G.C. Franzmeier, D.P. 1994. Clay mineralogy and chemistry of argillic horizons, fragipans, and paleosol B horizons of soils on loess-thinning transect in southwestern Indiana, USA. Geoderma 63, 77-93.

Van Reeuwijk, L.P. 2002. Procedures for Soil Analysis. Technical Paper n. 9. International Soil Reference and Information Centre, Wageningen, Netherlands.

Van Vliet, B. and Langohr, R. 1981. Correlation between fragipans and permafrost with special reference to silty Weichselian deposits in Belgium and Northern France. Catena 8, 137-153.

Wang, Y.H. and Siu, W.K. 2006. Structure characteristics and mechanical properties of kaolinite soils. I. Surface charges and structural characterizations. Canadian Geotechnical Journal 43, 587-600.

Wilson, M.J. 2004. Weathering of the primary rock-forming minerals: processes, products and rates. Clay Minerals 39, 233–266.

Wilson, M.A. Indorante, S.J. Lee, B.D. Follmer, L. Williams, D.R. Fitch, B.C. McCauley, W.M. Bathgate, J.D. Grimley, D.A. Kleinschmidt, K. 2010. Location and expression of fragic soil properties in a loess-covered landscape, Southern Illinois, USA. Geoderma 154, 529-543.

Witty, J.E. and Knox, E.G. 1989. Identification, role in soil taxonomy and worldwide distribution of fragipans. In: Smeck, N.E. Ciolkosz, E.J. (Eds.), Fragipans: Their Occurrence, Classification and Genesis. SSSA Spec. Publ. 24. SSSA, Madison, WI, 1-9.

Zhang, X.C. and Norton, L.D. 2002. Effect of exchangeable Mg on saturated hydraulic conductivity, disaggregation and clay dispersion of disturbed soils. Journal of Hydrology 260, 194-205.

Captions to Figures:

Figure 1. Location of the study area (A) and sketch of the soil profiles (B). The soil map is taken from IPLA (2009).

Figure 2. XRD pattern of oriented clay samples taken on the right (A) and left (B) river sides.

Figure 3. Clay mineral abundance in fragipan and non-fragipan samples on the right (A) and left (B) river side. The letters indicate significant differences between horizons (Tuckey test $p < 0.05$).

Table 1. Site characteristics.

Soil profiles	River side	Location	Coordinates	Elevation (m a.s.l.)	Land-use	Lithology
P1	Right	Fiano	45°13'25.8"N; 7°31'25.7"E	445	Natural forest and woodland	Ultramafic rocks
P2	Right	Grange di Fiano	45°12'08.4"N; 7°32'01.2"E	384	Natural forest and woodland	Ultramafic rocks
P3	Right	Robassomero	45°11'25.1"N; 7°34'24.9"E	357	Crops	Ultramafic rocks
P4	Left	Mathi	45°16'17.7"N; 7°32'37.4"E	438	Natural forest and woodland	Ultramafic and sialic metamorphic rocks
P5	Left	Vauda	45°16'09.5"N; 7°34'41.4"E	413	Natural forest and woodland	Ultramafic and sialic metamorphic rocks
P6	Left	San Francesco	45°13'46.0"N 7°40'37.8"E	310	Crops	Ultramafic and sialic metamorphic rocks

Table 2. Morphological properties of fragipan and non-fragipan B horizons.

Profile	Horizon	Boundary[1]	Munsell Colour	Mottles and concretions (% by vol.)	Soil structure[2]	Stickiness[3]	Plasticity[4]	Soil voids[5]
P1	Bw	10-30, GW	2.5 Y 6/6	2.5Y 2.5/1 (<2%)	SB, ME - CO	SST	SSP	F, V
	Bwg	30-60, DW	2.5 Y 7/4	2.5Y 2.5/1 (<2%); 7.5YR 6/8 (5%); 10YR 6/8 (5%)	SB, ME - CO	ST	SP	F, F
	Btc1	60-120, CW	10 Y 7/4	2.5Y 2.5/1 (5%); 10YR 6/3 (5%); 10YR 6/8 (10%); 5YR 5/8 (10%)	SB, ME - CO	ST	SP	V-F, V
	2Btc2	120-165, AS	10 Y 7/6	2.5Y 2.5/1 (10%); 5YR4/6 (15%); 5YR 4/3 (15%)	AB, ME - CO	ST	SP	V, V
	3Bcx	165-190, AS	10 YR 5/8	2.5Y 2.5/1 (10%); 7.5YR 6/8 (15%); 10YR 7/6 (15%)	AB-PL, ME - CO	ST	SP	V, V
	3Btcx	190-245, CS	10 YR 5/5	5YR 2.5/1 (20%); 2.5Y 7/1 (10%); 5YR 4/4 (20%)	AB-PL, ME - CO	VST	VSP	V, V
P2	Bw	25-40, GW	5 YR 4/6	-	SB, ME	ST	SP	F, V
	2Btx1	40-60, GW	5 YR 4/6	10YR 6/3 (20%)	AB, ME-CO	VST	VSP	F, F
	2Btx2	60-90, DW	5 YR 5/6	10YR 6/3 (15%); 10R 4/8 (15%)	AB, ME-CO	VST	SSP	F, F
	2Bcx1	90-110, GS	5 YR 5/8	10YR 6/3 (15%); 10R 4/8 (15%)	SB, CO	SST	SSP	V, V
	2Bcx2	110-130, GW	5 YR 5/8	10YR 6/3 (15%); 10R 4/8 (15%); 10YR 6/8 (10%)	SB, CO	NST	SSP	V, V
P3	Bw	30-50, CW	2.5 Y 5/6	2.5Y 5/2 (1%)	SB, ME - CO	SST	SSP	V, V
	Bwg	50-70, GW	2.5 Y 5/6	2.5Y 5/2 (<2%); 7.5YR 4/4 (<2%); 2.5Y 2.5/1 (<2%); 10YR 5/8 (5%)	SB, ME - CO	SST	SSP	V, V
	Bcx1	70-100, GW	2.5 Y 5/6	2.5Y 6/3 (30%); 10YR 5/6 (20%); 5YR 2.5/1 (<2%)	SB, ME - CO	ST	SP	V, V
	Bcx2	100-120, CW	2.5 Y 5/7	2.5Y 5/1 (20%); 5YR 2.5/1 (20%); 10YR 5/6(<20%)	SB, ME - CO	ST	SP	V, V
	Btx1	100-140, GW	10 YR 5/6	7.5YR 5/3 (10%); 5YR 3/3 (10%); 7.5YR 5/6 (15%)	AB, ME - CO	ST	SP	V, V
	Btx2	140-150, CW	10 YR 5/6	5YR 3/3 (5%); 7.5YR 5/1 (15%); 2.5YR 7/6 (5%); 10YR 6/8 (5%)	AB, ME - CO	ST	SP	V, V
	2Bcg1	150-175, GW	10 YR 5/6	5YR 3/3 (10%); 7.5YR 5/1 (20%); 2.5YR 7/6 (10%); 10YR 6/8 (10%)	SB, ME - CO	ST	SP	V, V
	2Bcg2	175-200+	10 YR 5/6	7.5YR 4/6 (10%); 10YR 6/8 (10%); 7.5YR 4/6 (10%); 7.5YR 2.5/1 (20%)	SB, ME - CO	ST	SP	V, V
P4	Bw	25-50, CS	7.5 YR 4/6	-	GR, VF	NST	NPL	V, V
	2Btx1	80-130, GS	5 YR 5/6	7.5YR 6/3 (5%); 2.5YR 4/6 (5%); 5YR 4/6 (5%)	SB, ME - CO	SST	SSP	V, V

	2Btx2	130-160, GS	10 YR 5/6	10YR 7/2 (20%); 5YR 5/6 (20%)	SB, ME - CO	ST	SP	F, V
	2Bcx	160-220+	5 YR 5/8	10YR 7/2 (20%); 2.5YR 4/6 (20%)	SB, ME - CO	ST	SP	V, V C
P5	2Btc	55-70, AS	10 YR 5/6	10YR 2/1 (5%); 7.5YR 4/3 (<5%)	AB, ME - CO	SST	SSP	F, V
	2Btx2	90-115, AS	10 YR 5/6	10YR 2/1 (10%); 7.5YR 4/3 (5%); 7.5YR 6/3 (5%)	AB-PL, ME - CO	ST	SP	V, V
	2Btx3	115-150, DW	10 YR 5/6	7.5YR 6/3 (5%); 10YR 2/1 (5%); 7.5YR 4/3 (20%); 7.5YR 6/8 (20%)	AB-PL, ME - CO	VST	VSP	V, V
	2Btx4	150-165, CW	7.5 YR 5/8	10YR 7/1 (5%); 10YR 2/1 (2%); 7.5YR 5/8 (50%)	AB-PL, ME - CO	ST	SP	V, V
	2Btx5	165-185, GW	5 YR 4/6	10YR 7/1 (20%); 10YR 2/1 (2%)	AB-PL, ME - CO	ST	SP	V, V
	3Btx6	185-225, GW	7.5 YR 5/6	10YR 7/1 (20%); 10YR 2/1 (2%); 5YR 4/6 (20%)	AB-PL, ME - CO	ST	SP	V, V
	3Btx7	225-240+	10 YR 5/8	10YR 7/1 (10%); 2.5YR 5/8 (40%)	AB-PL, ME - CO	SST	SSP	V, V
P6	Bw	10-50, DW	2.5 Y 5/4	7.5YR 4/4 (2%)	SB, CO	ST	SSP	V, V
	Bwg	50-100, CS	2.5 Y 5/4	10YR 5/2 (10%)	SB, CO	ST	SP	V, V
	2Bwx	100-120, AS	2.5 Y 5/6	10YR 5/2 (10%); 5YR 2.5/1 (20%); 5YR 3/3 (10%)	SB, CO	ST	SP	F, F
	3Btx	120-140, AS	10 YR 4/4	2.5YR 2.5/1 (5%); 5YR 3/3 (30%); 5YR 4/2 (5%)	AB, CO	ST	SP	F, F
	3Btg1	140-160, CS	10 YR 5/6	7.5YR 5/2 (20%); 2.5YR 2.5/1 (10%); 5YR 3/3 (25%)	AB, CO	VST	VSP	F, F
	3Btg2	160-180, CS	10 YR 5/6	7.5YR 4/4 (20%); 2.5YR 2.5/1 (10%); 5Y 5/1 (10%)	AB, CO	VST	VSP	F, F

[1] Upper – Lower boundary (cm), distinctness and topography. Distinctness: A = Abrupt, C = Clear, G = Gradual, D = Diffuse. Topography: W = Wavy, S = Smooth.
[2] Structure type, size class. Type: SB = Subangular blocky, AB = Angular blocky, GR = Granular, PL = Platy. Size class: ME = Medium, CO = Corse, VF = Very fine.
[3] Stickiness class: NST = Not sticky, SST = Slightly sticky, ST = Sticky, VST = Very sticky.
[4] Plasticity class: NPL = Not plastic, SPL = Slightly plastic, PL = Plastic, VPL = Very plastic.
[5] Pore diameter, abundance class. Voids diameter: V = Very fine, F = Fine, M = Medium, C = Corse. Pore abundance: V = Very few, F = Few, C = Common, M = Many.

Table 3. Soil chemical and geochemical properties and differences between fragipan (Bx) and non-fragipan (B) of the right and left river sides.

		Right river side								Left river side							
		B (n = 9)				Bx (n =10)				B (n = 6)				Bx (n = 11)			
		Min	Max	Mean	St. Dev	Min	Max	Mean	St. Dev	Min	Max	Mean	St. Dev	Min	Max	Mean	St. Dev
pH_{H2O}		4.8	6.8	5.7	0.6	4.9	6.6	5.8	0.6	5.2	6.5	6.1	0.5	5.5	6.5	6.0	0.3
OC	g Kg^{-1}	1.00	6.80	3.49^a	2.26	0.90	2.60	1.74^b	0.68	0.70	4.60	1.82	1.45	0.30	1.90	0.95	0.63
Clay	%	16.4	35.2	23.2^b	5.5	19.5	54.6	34.3^a	11.0	14.4	38.4	21.9	10.6	17.2	48.8	27.5	7.9
Silt	%	34.0	56.7	43.4^a	6.5	13.8	52.8	30.9^b	14.7	26.5	54.6	44.5	10.4	22.9	53.8	37.4	10.1
Sand	%	24.4	39.9	33.4	5.6	19.1	64.3	34.8	14.3	21.2	59.1	33.6	13.4	21.3	48.2	35.1	8.2
CEC	$cmol_{(+)}$ Kg^{-1}	9.3	15.6	12.0^b	2.4	8.2	23.8	16.8^a	4.7	6.0	24.7	15.5	7.4	10.3	19.9	14.0	3.0
Ca_{ex}	$cmol_{(+)}$ Kg^{-1}	1.15	4.83	3.20^b	1.21	3.03	6.67	5.12^a	1.20	0.69	8.14	4.40	3.20	1.75	6.46	3.17	1.69
Mg_{ex}	$cmol_{(+)}$ Kg^{-1}	0.82	5.55	2.73^b	1.91	2.06	6.99	4.67^a	1.63	1.03	11.52	6.07	4.53	2.67	8.23	4.13	2.04
K_{ex}	$cmol_{(+)}$ Kg^{-1}	0.05	0.07	0.06	0.00	0.06	0.11	0.07	0.01	0.02	0.11	0.08^a	0.03	0.02	0.09	0.05^b	0.02
BS[1]	$cmol_{(+)}$ Kg^{-1}	19.0	69.2	47.9	17.0	43.4	80.4	60.4	12.5	18.8	82.7	60.6	28.6	32.9	86.7	50.9	17.1
Fe_O	g Kg^{-1}	0.6	1.9	1.2	0.4	0.7	1.2	1.0	0.2	0.8	2.1	1.2	0.5	0.5	2.6	1.0	0.6
Fe_D	g Kg^{-1}	17.1	38.5	26.9^b	8.1	19.6	99.0	60.0^a	31.3	11.6	55.6	28.0	16.6	19.4	80.8	37.8	23.2
Fe_T	g Kg^{-1}	42.0	83.0	53.6^b	12.1	48.0	155.0	97.2^a	39.4	30.2	67.0	42.6	12.6	32.2	82.0	48.3	16.9
Fe_O/Fe_D		0.03	0.09	0.05^a	0.02	0.01	0.04	0.02^b	0.01	0.02	0.08	0.05	0.02	0.01	0.08	0.03	0.02
Fe_D/Fe_T		0.25	0.79	0.52	0.10	0.37	0.91	0.59	0.18	0.33	0.83	0.62	0.20	0.47	1.03	0.73	0.19
Mn_H	mg Kg^{-1}	36	600	277	217	2	700	158	210	53	305	212	88	5	1561	292	441
Mn_O	mg Kg^{-1}	43	648	329	239	3	2235	365	691	59	578	288	173	4	1775	313	502
Mn_D	mg Kg^{-1}	135	795	433	275	35	963	235	274	86	1005	415	310	25	2425	470	675
Mn_T	mg Kg^{-1}	195	850	492	262	72	980	296	273	155	1160	521	347	82	2975	594	818
Mn_I/ Mn_D		0.22	0.76	0.56	0.19	0.03	0.80	0.47	0.33	0.30	0.88	0.60	0.19	0.14	0.70	0.52	0.18
Mn_D/ Mn_T		0.57	0.97	0.83	0.14	0.49	0.98	0.70	0.13	0.56	0.89	0.76	0.12	0.24	0.91	0.72	0.20
Si_D	g Kg^{-1}	0.6	1.3	0.9^b	0.2	0.7	1.9	1.4^a	0.4	0.6	1.9	1.1	0.4	1.0	2.7	1.4	0.5
Al_O	g Kg^{-1}	1.2	1.9	1.4	0.3	1.0	1.9	1.4	0.3	1.0	2.0	1.5	0.3	0.9	1.6	1.2	0.2
EBS		0.20	0.38	0.26^b	0.06	0.21	0.64	0.37^a	0.14	0.16	0.41	0.24	0.11	0.18	0.53	0.30	0.09
ζ	mV	-18.0	-10.1	-15.1	2.5	-17.0	-12.2	-14.8	1.7	-21	-13	-17.5	2.7	-19.5	-9.5	-14.0	3.9

The letters indicate significant differences (Tuckey test $p < 0.05$).

[1] BS: Base saturation

Table 4. Results of the Discriminant Analysis performed using soil and clay characteristics on the right and left river sides.

River side	Discriminant functions[1]	Eigenvalues	% of explained variance	Canonical correlation coeff.	Wilks'lambda	p	Reclassification
Right	y = 1.31 Fe_D + 1.21 K	2.50	100	0.85	0.29	< 0.001	95%
	y = 0.81 (Int. min. 10-14) - 0.93 (Int. min. 14-14)	0.75	100	0.66	0.57	< 0.01	84%
Left	y = -1.55 CEC - 1.98 K	0.87	100	0.68	0.54	< 0.01	88%
	y = 1.43 Vermiculite - 0.78 Smectite + 1.17 (Int. min. 14-16) + 1.74 Kaolinite	5.61	100	0.96	0.15	< 0.001	100%

[1] Int. min. 10-14: Irregular interstratified illite-vermiculite or illite-chlorite minerals; Int. min. 14-14: Irregular interstratified chlorite-vermiculite minerals; Int. min. 14-16: Irregular interstratified swelling clay minerals (i.e. chlorite-smectite or vermiculite-smectite)

Table 5. Soil chemical, geochemical and mineralogical properties of fragipan (Bx) and non-fragipan (B) horizons of the whole study area and differences between B and Bx.

		B (n= 15)				Bx (n=21)			
		Min	Max	Mean	St. Dev	Min	Max	Mean	St. Dev
pH_{H2O}		4.8	6.8	5.9	0.6	4.8	6.5	5.9	0.5
OC	g Kg^{-1}	0.70	6.80	2.82[a]	2.09	0.30	2.60	1.33[b]	0.75
Clay	%	14.4	38.4	22.7[b]	7.6	17.2	54.6	30.8[a]	9.9
Silt	%	26.5	56.7	43.9[a]	7.9	13.8	53.8	34.3[b]	12.6
Sand	%	21.2	59.1	33.5	9.0	19.1	64.3	34.9	11.2
CEC	$cmol_{(+)}$ Kg^{-1}	6.0	24.7	13.4	5.1	8.2	23.8	15.3	4.1
Ca_{ex}	$cmol_{(+)}$ Kg^{-1}	0.69	8.14	3.75	2.23	1.75	6.67	4.10	1.76
Mg_{ex}	$cmol_{(+)}$ Kg^{-1}	0.82	11.52	4.07	3.50	2.06	8.23	4.39	1.83
K_{ex}	$cmol_{(+)}$ Kg^{-1}	0.02	0.11	0.07	0.02	0.02	0.11	0.06	0.02
BS[1]	$cmol_{(+)}$ Kg^{-1}	18.8	82.7	53.0	22.3	32.9	86.7	55.4	15.5
Fe_O	g Kg^{-1}	0.6	2.1	1.2	0.4	0.5	2.6	1.0	0.4
Fe_D	g Kg^{-1}	11.6	55.6	27.4	11.6	19.4	99.0	48.4	28.9
Fe_T	g Kg^{-1}	30.2	83.0	49.2	13.2	32.2	155.0	71.6	38.3
Fe_O/Fe_D		0.02	0.09	0.05[a]	0.02	0.00	0.07	0.03[b]	0.01
Fe_D/Fe_T		0.25	0.83	0.56	0.18	0.36	1.03	0.66	0.19
Mn_H	mg Kg^{-1}	36	600	251	175	2	1561	228	349
Mn_O	mg Kg^{-1}	43	648	313	210	3	2235	338	584
Mn_D	mg Kg^{-1}	86	1005	425	279	25	2425	358	525
Mn_T	mg Kg^{-1}	155	1160	503	287	72	2975	452	626
Mn_I/ Mn_D		0.22	0.87	0.58	0.18	0.03	0.79	0.50	0.26
Mn_D/ Mn_T		0.55	0.97	0.80	0.13	0.24	0.98	0.71	0.16
Si_D	g Kg^{-1}	0.6	1.9	1.0[b]	0.3	0.7	2.7	1.4[a]	0.4
Al_O	g Kg^{-1}	1.0	2.1	1.4	0.3	0.9	1.8	1.3	0.3
EBS		0.16	0.41	0.25	0.08	0.18	0.64	0.33	0.12
ζ	mV	-20.6	-10.1	-16.0	2.8	-19.5	-9.5	-14.4	3.0

The letters indicate significant differences (Tuckey test $p < 0.05$).

[1] BS: Base saturation

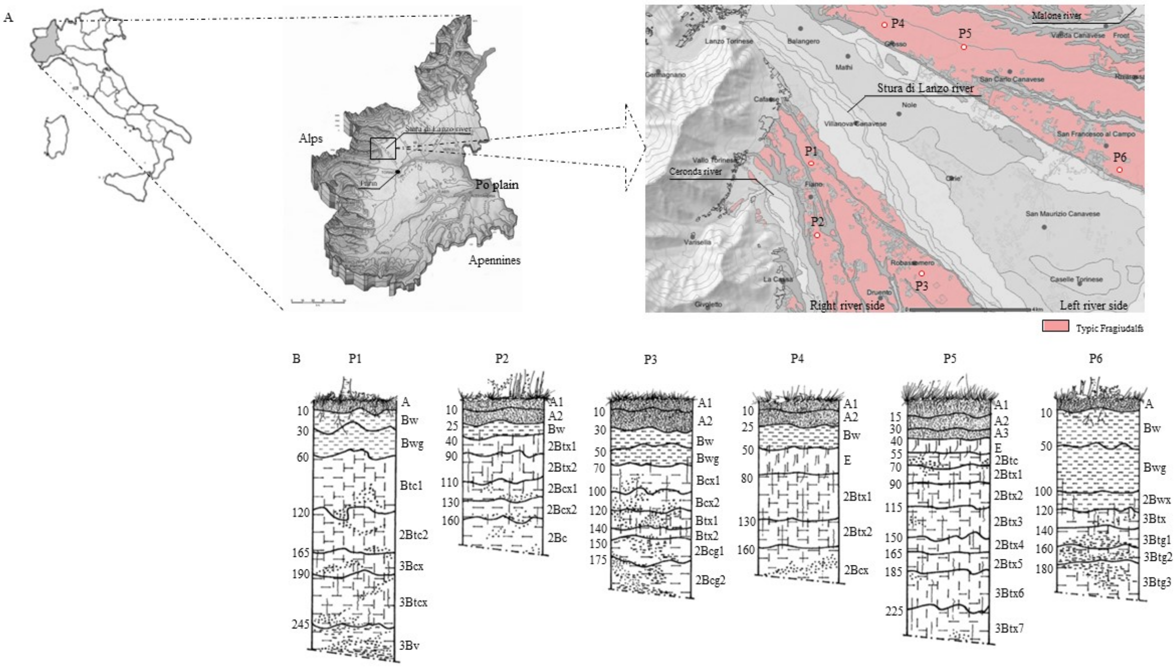
A
Alps
Po plain
Apennines
Stura di Lanzo river
Ceronda river
Malone river
P1
P2
P3
P4
P5
P6
Right river side
Left river side
Typic Fragiudalfs
B

Figure 1

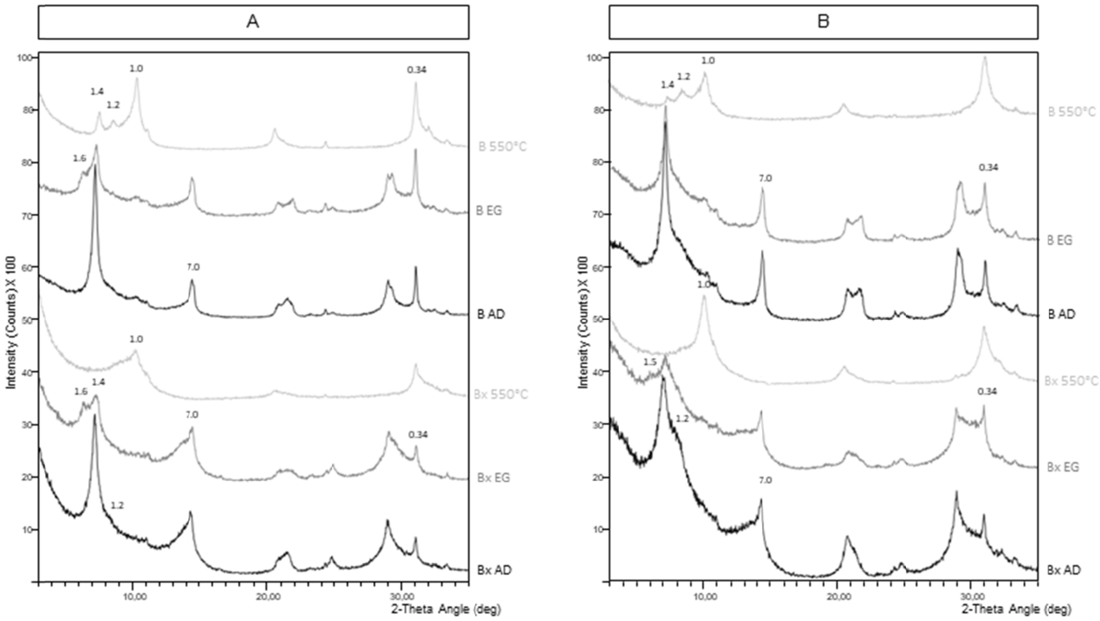
A
B
Intensity (Counts) X 100
2-Theta Angle (deg)
B 550°C
B EG
B AD
Bx 550°C
Bx EG
Bx AD
1.6
1.4
1.2
1.0
7.0
0.34
1.5

Figure 2

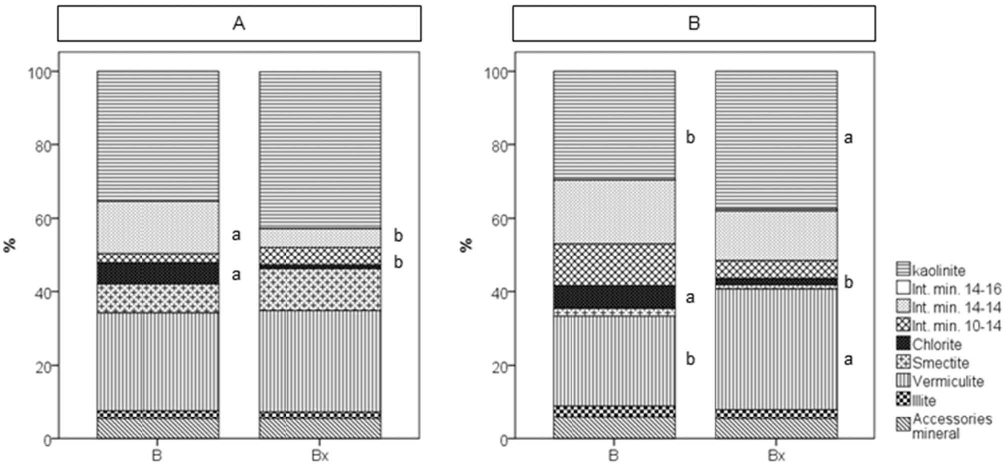
A
B
%
100
80
60
40
20
0
a
b
a
b
B
Bx
b
a
a
b
b
a
kaolinite
Int. min. 14-16
Int. min. 14-14
Int. min. 10-14
Chlorite
Smectite
Vermiculite
Illite
Accessories mineral

Figure 3